HHS Public Access

Author manuscript

J Immunol. Author manuscript; available in PMC 2016 May 01.

Published in final edited form as:

J Immunol. 2015 May 1; 194(9): 4555–4566. doi:10.4049/jimmunol.1402734.

SNX17 Affects T Cell Activation by Regulating T Cell Receptor and Integrin Recycling

Douglas G. Osborne[1,*], **Joshua T. Piotrowski**[1], **Christopher J. Dick**[1], **Jin-San Zhang**[1], and **Daniel D. Billadeau**[1]

[1]Departments of Immunology and Biochemistry and Molecular Biology, Division of Oncology Research and Schulze Center for Novel Therapeutics, Mayo Clinic College of Medicine, Rochester, MN 55905, USA

Abstract

A key component in T cell activation is the endosomal recycling of receptors to the cell surface, thereby allowing continual integration of signaling and antigen recognition. One protein potentially involved in T cell receptor transport is sorting nexin 17 (SNX17). SNX proteins have been found to bind proteins involved in T cell activation, but specifically the role of SNX17 in receptor recycling and T cell activation is unknown. Using immunofluorescence, we find that SNX17 co-localizes with TCR and localizes to the immune synapse in T-APC conjugates. Significantly, knockdown of the SNX17 resulted in fewer T-APC conjugates, lower CD69, TCR, and LFA-1 surface expression, as well as lower overall TCR recycling compared to control T cells. Lastly, we identified the FERM-domain of SNX17 as being responsible in the binding and trafficking of TCR and LFA-1 to the cell surface. These data suggest that SNX17 plays a role in the maintenance of normal surface levels of activating receptors and integrins to permit optimum T cell activation at the immune synapse.

Keywords

SNX17; TCR; LFA-1; CD4$^+$ T cells; receptor trafficking; lysosomes

Introduction

Interactions between CD4$^+$ T lymphocytes and antigen presenting cells (APCs) leads to the spatial redistribution and reorganization of specific adhesion and signaling receptors at the T-APC interface leading to the formation of the immunological synapse (IS) (1, 2). The key to sustaining the IS, and thus T cell activation, is the continual turnover (3, 4) and vesicular/endosomal transport (5–7) of specific adhesion and signaling receptors to the IS. The TCR requires endosomal transport and recycling before and during IS formation, to help sustain both the synapse and signaling (5, 8). The mechanism of TCR transport and recycling at the IS during T cell activation has been reported to involve several Rab family GTPases (5, 9–11), the t-SNAREs: VAMP-3 (8), ti-VAMP (5, 12), the intraflagellar transport (IFT) system

To whom correspondence should be addressed. billadeau.daniel@mayo.edu; Phone: (507) 266-4334; Fax: (507) 266-5146.

protein IFT20 (9) and the ARP2/3 activating Wiskott-Aldrich Syndrome Protein and SCAR Homolog (WASH) complex (13).

One group of proteins involved in the sorting of receptors from early endosomes to the plasma membrane are sorting nexins (SNX) (14, 15). Thirty-one of the 33 SNX proteins contain a phox-homology (PX) domain, which bind phosphoinositides on endosomal membranes (14, 15). In general, the remainder of the SNX protein is used in the binding and sorting of receptors for transport out of the endosomal system (14–16). Three SNX proteins: SNX17, SNX27, and SNX31 contain a 4.1/ezrin/radixin/moesin (FERM)-like domain (17) shown to be involved in retrieval and recycling of several receptors and integrins containing an Asn-Pro-Xaa-Tyr (NPxY) motif (18–22). SNX17 has been to shown to play an important role in the prevention of lysosomal degradation of NPxY-motif containing β_1-integrin (23, 24), LDL receptor (20, 21) and P-selectin (25). SNX27 was shown to interact with T cell signaling molecules, such as diacylglycerol kinase ζ, at the immune synapse (26). However, little is known about the role of FERM-domain containing sorting nexins in T lymphocyte receptor trafficking and activation.

Here we show that SNX17 participates in the sorting and transport of TCR and LFA-1 in human $CD4^+$ T cells. Using 3D confocal microscopy, we find that SNX17 localizes with the TCR at the immune synapse. Consistent with a role for this protein in regulating the trafficking of cell membrane receptors, we find decreased TCR and LFA-1 surface expression when SNX17 is depleted in either primary human $CD4^+$ T cells or Jurkat T cell. Functionally, the loss of SNX17 impacts both T cell activation and conjugate formation. Finally, we show that SNX17 interacts with both CD3ε and CD18 and this interaction requires the SNX17 FERM-domain. Overall, these data demonstrate the importance of SNX17 in T cell activation through its transport effects on both TCR and LFA-1.

Materials and Methods

Cell lines and transfections

Jurkat T cells (human acute T cell leukemia), Raji cells (human Burkitt's lymphoma), and primary human $CD4^+$ T cells were used for all experiments. Primary human $CD4^+$ T cells were purified from whole blood cones using RosetteSep human $CD4^+$ T cell enrichment cocktail (Stemcell Technologies) and hypotonic lysis, then placed in culture for four days and supplemented with 10 U/ml IL-2. All cells were cultured in "complete RPMI 1640" containing RPMI 1640 medium (Life Technologies) supplemented with 5% FBS (Atlanta Biologicals), 5% BCS (Thermo), and 1 mM L-glutamine. Transfection of Jurkat T cells took place during logarithmic growth phase using siRNA or short hairpin RNA constructs. For siRNA, 10^7 Jurkat T cells or primary human $CD4^+$ T cells were placed in a 100 μl nucleofection solution with 300 pMol siRNA against SNX17 sequence (5′-CAUUCACGUGAAUGGAGUC(dTdT)-3′) using AMAXA nucleofection (Life Technologies). A lentivirus expressing an shSNX17 target sequence (5′-CGTATCCTACCTTTCCTTG-3′) was used to infect Jurkat T cells. A bulk population of infected cells was obtained following puromycin selection and used for experiments. Additionally, we generated a suppression/re-expression vector to simultaneously deplete SXN17 using a 3′UTR sequence (5′-CGTATCCTACCTTTCCTTG-3′) and re-express either

HA-YFP fused wild type SNX17 or L353W FERM domain mutant (forward primer: 5′-GGCTTTGAATACTGGATGAGCAAGGACC-3′ and reverse primer: 5′-GCTTGCAGTCCATGGATGAACTGATGG-3′). Jurkat T cells were electroporated with 40 μg of the indicated plasmids in 4 mm gap cuvettes using a BTX electro square porator (ECM 830). We used YFP expression to gate on the transfected Jurkat T cell population for the indicated experiments.

Antibodies and staining reagents

The following conjugated and unconjugated Abs were purchased from BD Biosciences: anti-αβTCR (clone IP26), anti-CD11a (G43-25B), anti-ZAP70 ((PY319)/Syk (PY353); clone 17A/P-ZAP70), anti-CD69 (clone L78), anti-CD18 (M18/2), and anti-CD4 (clone L200). Conjugated antibody for anti-αβTCR (clone IP26) was purchased from eBiosciences. Rabbit polyclonal Abs specific for LAMP1 (ab24170) purchased from Abcam and specific for SNX17, CD3ε, and CD18 were purchased from Protein Tech Group. Mouse monoclonal and goat polyclonal Abs specific for SNX17 (clones H-10 and N-14) and a mouse monoclonal Ab specific for TCR (clone G-11) were purchased from Santa Cruz. Secondary staining reagents including Alexa Fluor-633 conjugated donkey anti-goat IgG, Alexa Fluor-488 conjugated goat anti-hamster IgG, Alexa Fluor 568-conjugated donkey anti-rabbit IgG, Alexa Fluor-568 conjugated donkey anti-mouse IgG, and Alexa Fluor-633 conjugated goat anti-mouse and goat anti-rabbit IgG were purchased from Life Technologies.

Flow cytometry: TCR and LFA-1 surface expression

Jurkat T cells and primary human $CD4^+$ T cells were removed from cultures and resuspended at 10^6 cells/ml in FACS buffer (pH 7.4 PBS containing 2% BSA Fraction V [Sigma] and 0.1% NaN_3). Cells were stained for 30 min at 4°C with anti-TCRαβ-APC (eBiosciences and BD Biosciences), anti-CD11a-PE (BD Biosciences), and anti-CD18-PE (eBiosciences) or the indicated fluorescently conjugated antibody. After a wash in FACS buffer, cells were resuspended in 500 μl FACS buffer and analyzed using flow cytometry using a FACSCanto II flow cytometer (BD Biosciences). Data were analyzed using FlowJo 8.8.7 software (Tree Star, Ashland, OR).

T cell stimulation and drug treatment (cycloheximide and bafilomycin A1)

To measure and compare changes in TCR and LFA-1 surface expression on active $CD4^+$ SNX17 knockdown T cells we used antibody stimulation. Either Jurkat T cells or primary human $CD4^+$ T cells were treated with 5 μg/ml anti-TCR (clone OKT3) and anti-CD28 (clone CD28.2) for 30 min at 4°C in FACS buffer + %5 FBS. Following a single wash in FACS buffer, cells were treated with 10 μg/ml goat anti-mouse secondary for 20 min at 4°C to crosslink the TCR. After two washes in 1X PBS, cells were resuspended at 10^6 cells/ml in complete medium for 2.5 hrs, washed in FACS, stained and prepared for flow cytometry or immunofluorescence (IF). To measure if TCR or LFA-1 surface expression differences are due to changes in protein expression in WT and knockdown T cells, cells were treated with 20 μg/ml cycloheximide (Sigma) for 24hrs in complete medium. Following treatment, cells were washed in FACS buffer and prepared for flow cytometry or IF. Or to measure if TCR or LFA-1 expression differences are due to lysosomal degradation in WT and knockdown T cells, cells were treated with 100 nM bafilomycin A1 (Sigma) for 18hrs in complete

medium. Following treatment, cells were fixed by the addition of 4% paraformaldehyde (PFA) in 1X PBS and incubated for 15 min at room temperature, followed by permeabilization with 0.2% Triton X-100 in PBS for 3 min, washed in FACS buffer and prepared for flow cytometry.

Conjugate assay

10^7 Jurkat T cells were labeled with 10 mM CMAC7 at 37°C for 30 min in covered dH_20 water bath and Raji cells target cells were labeled for 30 min at 37°C with 1 μM carboxyfluorescein succinimidyl ester (CFSE). Labeled Jurkat T cells and Raji B cells were then washed and resuspended at 10^6 cells/ml. Raji B cells were then loaded with/without 10 ng/ml Staphylococcal enterotoxin E (SEE) superantigen and incubated for at least 60 min at 37°C Cells (500 μl each) and mixed together with Jurkat T cells and centrifuged, and allowed to incubate at 37°C for up to 60 min with aliquots taken at 0, 5, 10, 25, 40, and 60 min, and vortexed vigorously for 20 sec before fixing with 4% PFA. Conjugate formation was assessed using two color flow cytometry and is revealed by dual emission of blue (Raji) and green (Jurkat) fluorescence. Concurrently conjugate samples were taken at each time point and stained for surface expression of CD69 and fixed (4% PFA) and permeabilized using ice-cold 50% methanol in 1X PBS to assess the phosphorylation state of ZAP-70 in $green^+$ cells.

Immunofluorescence (IF)

Jurkat T cells or primary human $CD4^+$ T cells were cultured on poly-L-lysine coated #1.5 LabTek II eight-chambered coverslips (Nunc) for at least 30 min to allow firm adhesion. For synapse imaging, primary human $CD4^+$ T cells were placed in co-culture with CMAC7 stained SE cocktail (10 ng/ml of each SEA, SEB, SEC, and SEE antigen) loaded Raji cells for 30 min prior to plating on pol-L-lysine coated coverslips. Cells were fixed by addition of ice-cold fixative (4% paraformaldehyde and 0.5% glutaraldehyde in PBS) and incubated for 30 min at room temperature in the dark, followed by permeabilization with 0.2% Triton X-100 in PBS for 15 min. Cells were then cultured with 10 μg/ml primary antibodies (Abs) in IF buffer (TBS plus human serum cocktail) overnight at 4°C in a humidifier chamber. Following 5–6 washes in PBS, cells were incubated with secondary Abs (1:500 dilution in imaging buffer) for 1 hr at room temperature. After 5–6 washes with PBS and addition of Hoechst 33342 nuclear stain, SlowFade Gold antifade reagent (Molecular Probes) was added to the wells. Images were obtained with an LSM-710 laser scanning confocal microscope with a 100X/1.4 Oil Plan-Aprochromat objective lens using ZEN software (Carl Zeiss). Each image represents an individual slice taken from a z-stack comprised of several slices at 0.25 μm depth.

Endocytosis assay

To specifically track the localization of surface-derived TCR or LFA-1 after endocytosis, we performed an IF directed endocytosis assay. siControl or siSNX17 primary human $CD4^+$ T cells or shControl or shSNX17 Jurkat T cells were cultured on #1.5 LabTek II eight-chambered coverslips as described above. After 30 min culture, the cell media was replaced with serum-free DMEM containing 10 μg/ml anti-TCR (Biolegend) or anti-CD11a (BD

Biosciences) and then incubated at 37°C for 30 min to allow internalization. Cells were then prepared for IF using the protocol described above.

Image Analysis

Co-localization was assessed by Pearson's correlation coefficient and overlap coefficient using ZEN software (Carl Zeiss) or FIJI (National Institutes of Health: http;// rsb.info.nih.gov/ij/). Mean fluorescence intensity (MFI) and puncta number were measured using 3D z-stack images at 0.25 μm slice spacing together with the *Analyze Particles* feature in FIJI. Line intensity profiles were created using *Surface plot* in FIJI to measure differences in fluorescence across a cell and at the synapse by drawing a line from the distal part of cell membrane, directly opposite of the synapse, to and across the synapse and then data was entered into Prism 4 (GraphPad Software). Co-localization of SNX17 with TCR at the distal or synaptic membrane was measured using a region of interest (ROI) that encompassed the synapse between two cells or the distal membrane (directly opposite the synapse) and assessed by the overlap coefficient using ZEN software.

Receptor recycling assay

Vector control or SNX17 KD Jurkat T cells or primary human T cells were surfaced labeled with an anti-TCRαβ-APC (BD Biosciences) or an anti-CD11a-PE (BD Biosciences) antibody for 30 min, washed in complete RPMI 1640 and incubated for 30 min to allow antibody internalization. Cells were then spun down and resuspended in FACS buffer stripping solution (PBS containing 2% BSA Fraction V and 0.1% NaN_3, pH 2.5) for 10 min on ice and washed in stripping solution. Cells were then washed in cold FACS buffer (pH 7.4 PBS containing 2% BSA Fraction V [Sigma Aldrich] and 0.1% NaN_3) and resuspended in complete RPMI. Resuspended T cells were then incubated for 0, 10, 20 and 40 min to allow resurfacing of the internalized TCRαβ or CD11a. Following incubation, cells again were spun down and resuspended in FACS buffer stripping solution for 10 min on ice and washed in stripping solution. Cells were then washed, resuspended in 500 μl FACS buffer and analyzed by flow cytometry. Data were analyzed using FlowJo 8.8.7 software. The percentage of recycled TCR or CD11a was measured using the equation $(T_0 - T_x)/T_0 \times 100$. T_0 represents the mean fluorescence of cells following the second acid strip at time zero and T_x is the mean fluorescence intensity of cells stripped at each time point. The acid stripping method was adapted from (27).

GST pull-down assay

Pull-down assays using GST-SNX17 and GST-SNX17 (L353W) mutant were performed as previously described (28). Pull-down assays were performed using a total of 5 μg GST fusion protein bound to GSH-agarose. The GST-bound fusion protein was incubated with 1 mg of clarified lysate prepared from unstimulated or anti-CD3/CD28-stimulated T cells. Samples were then prepared for immunoblot with anti-CD3ε or CD18 antibody (Rabbit polyclonal 1:1000). Alternatively, the GST-bound fusion protein was directly incubated with MBP-fused cytoplasmic domains from CD3ε or CD18 in 500 μl pull-down buffer (PB: 1 M HEPES [pH 7.2], 50 mM CH3CO2K, 1 mM EDTA, 200 mM D-sorbitol, 0.1% Triton X-100, 1 mM PMSF, 10 mg/ml leupeptin, and 5 mg/ml aprotinin). The protein complexes

were incubated at 4°C and then washed twice with PB. Approximately 90–95% of precipitated samples were subjected to coomassie staining and 5–10% for immunoblot with anti-MBP antibody (Rabbit polyclonal 1: 2000).

Statistical Methods

Data are expressed throughout as mean ± standard error mean. Data sets were compared using the two-tailed unpaired Student's t-test. Statistical analysis (Student's t-test and column statistics) and graphing were performed using Prism 4. Differences were considered statistically significant when $p<0.05$.

Results

SNX17 localizes with TCR and LFA-1 in Jurkat T cells

The sorting nexin FERM-domain binds specifically to NPxY/NxxY/NPxF motifs on other proteins for their transport and recycling (18, 20–22, 24, 25), suggesting that the cytoplasmic tails of receptors expressed in T cells that bear this motif, such as the TCR and LFA-1, could be targets of SNX17. To initially determine if an association exists between SNX17 and the TCR and LFA-1, we used 3D confocal microscopy, and an endocytosis assay where we surface labeled the cell with antibodies against the TCR or CD11a (α-chain of LFA-1), then placed the cells in culture at 37°C for 30 min to allow internalization of the antibody. This allowed us to monitor surface receptor localization in the cells following endocytosis. We initially confirmed that SNX17 localizes to endosomes (24) using antibodies against the early endosome marker early endosomal antigen-1 (EEA1) (Supplemental Fig. S1A). SNX17 localization to endosomes is confirmed by the relatively high co-localization with EEA1 (Supplemental Fig. S1B). In Fig. 1A, Jurkat T cells were left unstimulated (top) or were stimulated (bottom) using anti-CD3 and CD28 ligation, to determine if there is a difference in SNX17/TCR localization when the cells were stimulated. Both unstimulated (top) and stimulated (bottom) Jurkat T cells show similar co-localization of SNX17 (red) with TCR (green) throughout the cells. Using ZEN software, co-localization is confirmed between SNX17 and TCR using Pearson's co-localization coefficient (Fig. 1B), with a significant increase in co-localization following stimulation. Like SNX17, the TCR was also found to localize to early endosomes in the cytosol as shown by SNX17, TCR, and EEA1 staining (Supplemental Fig. S1A). We also imaged unstimulated and antibody-stimulated primary human $CD4^+$ T cells to determine if there are any differences in SNX17 localization with the TCR compared to Jurkat T cells, and found that SNX17 co-localized with the TCR (Fig. 1C) in both unstimulated and stimulated primary T cells, and again there is a significant increase in co-localization when the T cells were stimulated (Fig. 1D).

We next examined the localization of SNX17 with CD11a in antibody-stimulated and unstimulated Jurkat T cells. SNX17 has been shown to participate in integrin transport (23, 24) but not specifically in T cell integrin transport. Supplemental Fig. S1C shows the localization of SNX17 with CD11a in unstimulated or stimulated Jurkat T cells. The stimulated Jurkat T cells (bottom) appear to contain increased co-localization of SNX17 with CD11a (demarcated by yellow puncta), than unstimulated cells (top). Consistent with this observation, the co-localization coefficient between SNX17 and CD11a doubles from

0.37 to 0.75 when the T cells are activated (Supplemental Fig. S1D). These data suggest that TCR ligation regulates SNX17 localization with CD11a but may play less of a role in the localization of SNX17 with the TCR on early endosomes.

SNX17 depletion affects T cell surface expression of TCR and LFA-1

To explore the role of SNX17 in T cell activation and to determine if TCR and LFA-1 surface expression is dependent on SNX17, we depleted SNX17 in both primary human $CD4^+$ T cells and Jurkat T cells using siRNA and lentiviral shRNA, respectively. Significantly, compared to control cells, SNX17-depleted Jurkat T cells (Fig. 2A, top panels) showed a mark reduction in cell surface expressed TCR and CD11a (Fig. 2B) using flow cytometry. Next we analyzed TCR expression in siSNX17 primary human $CD4^+$ T cells (Fig. 2A, bottom panels) again using flow cytometry. Both unstimulated and stimulated siControl T cells have a ~60% higher TCR MFI than siSNX17 T cells (Fig. 2C, left). The siControl T cells also have a greater than 2-fold decrease in TCR MFI when stimulated, which can be attributed to TCR-downmodulation (3). There is also ~3-fold decrease in TCR MFI when siSNX17 T cells are stimulated (Fig. 2C, left). Thus, TCR can be downmodulated upon activation, but prior to activation there is a substantial loss of cell surface TCR. Furthermore, siSNX17 stimulated primary human $CD4^+$ T cells have a nearly 2-fold decrease in CD11a expression (Fig. 2C, center) and an ~29% decrease in CD18 surface expression (Fig. 2C, right). No significant difference in CD11a and CD18 expression is seen in unstimulated T cells (Fig. 2C, center and right). These data, along with the images in supplemental Fig. S1C, suggest that SNX17 transport of LFA-1 is dependent on T cell stimulation. To determine if SNX17 loss impacts other receptors involved in T cells activation, we monitored the surface expression of the co-receptor CD4 and costimulatory receptor CD28, which are absent of potential FERM binding domains. As shown in Supplemental Fig. S2A, no significant difference in CD4 or CD28 surface expression is seen between siControl and siSNX17 primary human T cells regardless of cell stimulation. Taken together, these data suggest that SNX17 is involved in TCR and LFA-1 receptor trafficking, and SNX17 transport of LFA-1 is more reliant on TCR-stimulation, which might impact T cell activation.

SNX17 depletion impacts conjugate formation and T cell activation

Having lower TCR and LFA-1 on the T cell surface of SNX17-depleted cells would suggest that these cells should also have diminished ability to interact with APCs, and thus, decreased activation. Using superantigen loaded Raji cells, we next examined the ability of SNX17-depleted Jurkat T cells to form conjugates and become activated. Following the protocol shown in Fig. 3A, we placed +SEE loaded $CFSE^+$ Raji cells and $CMAC7^+$ Jurkat T cells in culture together over a 60-min time course and measured the amount $CFSE^+CMAC7^+$ conjugates formed using flow cytometry. For all time points analyzed, the shControl cells showed significantly higher conjugate formation compared to shSNX17 cells (Fig. 3B). In fact, the percentage of conjugates is ~3 fold higher for shControl cells than shSNX17 cells. The contour plots (Fig. 3B, bottom) for the 40 min time point, show that 10.3% of the shControl Jurkat T cells formed conjugates while only 4.28% of the shSNX17 Jurkat T cells formed conjugates. The lower conjugate formation by SNX17-depleted cells is consistent with these cells having lower surface integrin and TCR levels.

We also measured the level of T cell activation and TCR signaling following the loss of SNX17. To measure T cell activation differences between shControl and shSNX17 cells, we examined the expression of the early activation marker CD69 and the phosphorylation of the tyrosine kinase ZAP-70 for all CMAC7$^+$ cells including cells in conjugate with Raji cells. At time 0 and in unstimulated (resting) Jurkat T cell cultures, the shSNX17 cells have half the amount of CD69 on their surface (Fig. 3C, top). When the Jurkat T cells were placed in culture with SEE-loaded Raji cells for 30 to 60 min, the level of CD69 increased in shControl cells, but decreased in shSNX17 cells. It is unknown whether the trafficking of CD69 is SNX17-dependent, but CD69 does not contain an identifiable NPxY motif. Consistent with their being a defect in activation of shSNX17 cells, pZAP70 increased over the course of stimulation in shControl cells but decreased in the shSNX17 cells (Fig. 3C, bottom). For each time point shown in Fig. 3C, the pZAP-70 MFI levels in the shSNX17 cells are around 600 MFI and do not vary in significance. Overall, the results shown in Figures 1–3 demonstrate that SNX17 localizes with TCR and LFA-1, and participates in the surface expression of these receptors, ultimately impacting T cell activation.

SNX17 prevents TCR trafficking to and degradation in the lysosomes

Previous results examining WASH protein function has shown that immune cells lacking WASH accumulated and degraded receptors in lysosomes (13). If SNX17, like WASH, regulates the recycling of LFA-1 and TCR back to the cell surface, we might expect to see receptors accumulate with lysosomes upon SNX17 depletion. In Fig. 4A, we used IF to monitor the localization of SNX17, TCR, and lysosomal acid membrane protein 1 (LAMP1) in antibody-activated primary human CD4$^+$ T cells. Representative images show that SNX17 and TCR staining overlap significantly, consistent with the co-localization data shown in Fig. 1D. However, while SNX17 and TCR are co-localized, LAMP1 is noticeably absent from the co-localized puncta (Fig. 4A, zoom merge). In contrast, TCR can be seen co-localizing with LAMP1 in siSNX17 cells (Fig. 4A zoom merge). Analysis of the TCR and LAMP1 puncta confirms that in the absence of SNX17, TCR puncta MFI are lower and TCR co-localization with LAMP1 in large intracellular puncta increases significantly (Fig. 4A, graphs). These data were also confirmed in shControl and shSNX17 Jurkat T cells (Supplemental Fig. S2B–D).

Upon examining CD11a, we noted that in stimulated siControl T cells, SNX17 is co-localized with CD11a consistent with the results in Supplemental Fig. S1C & S1D, and LAMP1 is absent from the SNX17-CD11a co-localized puncta. However, in stimulated siSNX17 T cells, there is a significant increase in CD11a co-localization with LAMP1 (Fig. 4B zoom merge), which was confirmed by overlap coefficient showing a 2-fold increase in CD11a-LAMP1 co-localization when SNX17 is removed (Fig. 4B, graphs). Taken together these data suggest that SNX17 prevents TCR and LFA-1 lysosomal accumulation.

We next examined whether the increased lysosomal localization seen in the absence of SNX17 was leading to increased degradation of the receptors in the lysosome. To determine if the loss of receptor expression is due to increased lysosomal degradation, we examined the MFI of TCR in siControl and siSNX17 primary human CD4$^+$ T cells treated with bafilomycin A1, an inhibitor of lysosomal function. Cells were fixed and permeabilized to

measure total protein, not exclusively surface level expression. As can be seen in Fig. 4C left, siSNX17 T cells have ~30% decreased total TCR levels compared to siControl T cells. However, the addition of bafilomycin A1 restores total TCR MFI levels to that of siControl cells. Restoration of TCR levels were similarly observed in shSNX17 Jurkat T cells treated with bafilomycin A1 (Supplemental Fig. S3A). We also noted that treatment of shSNX17 Jurkat T cells with bafilomycin A1 restored CD11a levels to those of shControl cells (Fig. 4C, right). These data indicate that SNX17 prevents the lysosomal degradation of both TCR and LFA-1.

SNX17 is involved in receptor recycling in T cells

The localization of SNX17 with the TCR near the cell surface (Fig. 1 and 4) suggested a potential role in the trafficking of the TCR from the endosomal network back to the cell surface. To investigate this, we used the protein translation inhibitor, cycloheximide (CHX), to determine whether the loss of TCR and LFA-1 surface expression in SNX17-deficient T cells is due to a defect in receptor trafficking or protein expression. Antibody stimulated siControl or siSNX17 human $CD4^+$ T cells were treated with 20 μg/ml CHX for 24 hrs, antibody stained for TCR and LFA-1, and analyzed by flow cytometry. Control T cells without CHX had a ~2-fold higher TCR MFI than siSNX17 T cells, confirming earlier results (Fig. 2B and 2C), but when treated with CHX both siControl and siSNX17 T cells showed a decrease in TCR MFI (~25% for siControl and ~40% for siSNX17) compared to untreated cells (Fig. 5A). The decreased TCR MFI in siControl cells is expected due to inhibition of TCR synthesis by CHX; but the decrease in TCR MFI in siSNX17 T cells is significant for it shows the lower TCR surface expression on untreated siSNX17 cells is not merely due to a decrease in protein synthesis. Using antibody staining against CD11a, we found that untreated siControl cells have a ~3-fold higher CD11a MFI than untreated siSNX17 cells (Fig. 5B). Treatment with CHX lead to decreases in CD11a MFI for both siControl (~35%) and siSNX17 (~40%) T cells. Again, the ~40% decrease in CD11a MFI in siSNX17 cells when treated with CHX suggests that SNX17 is involved in the recycling of these two proteins back to the cell surface.

To determine if SNX17 is directly involved in receptor recycling, we used a recycling assay adapted from Sullivan *et al*. (27). Primary human $CD4^+$ T cells were surface stained for TCR or CD11a. Following surface labeling, the cells were incubated to allow for antibody internalization, acid stripped, then incubated for different time points to allow for reemergence of internalized antibody and acid stripped again. Following the equation $(T_0 - T_x)/T_0 \times 100$ from the Materials and Methods, we were able to determine the percentage of receptor recycling over the 40 min time course by flow cytometry. If recycling remains intact, the internalized antibody will return to the surface and be removed by the acid stripping buffer, leading to a reduction in fluorescence. As expected, regardless of cell activation, primary human T cells exhibited a reduction in TCR fluorescence over the time course, indicative of TCR recycling (Fig. 5C). In contrast, SNX17-deficient cells demonstrated a minimal reduction in TCR fluorescence and essentially no recycling even after stimulation (Fig. 5C). Similarly, CD11a recycling was unaffected by stimulation, but depletion of SNX17 lead to a near complete loss of CD11a recycling under stimulated or unstimulated conditions (Fig. 5D). Interestingly, there is still some recycling of CD11a in

unstimulated SNX17-deficient T cells, suggesting there are other pathways independent of SNX17 for CD11a transport in unstimulated T cells. However, when stimulated, CD11a recycling becomes increasingly dependent on SNX17 transport. Similar defects in TCR and CD11a recycling were observed in SNX17-depleted Jurkat T cells (Fig. S3B). These data identify a clear role for SNX17 in the regulation of TCR and CD11a recycling.

SNX17 co-localizes with TCR in primary human CD4$^+$ T cells at the immune synapse

SNX17 and TCR localize together in CD4$^+$ T cells and with the loss of SNX17 there is decreased TCR expression, TCR recycling, conjugate formation, and activation, which suggests a possible role for SNX17 at the immune synapse. We therefore examined the localization of SNX17 in primary human CD4$^+$ T cells in coculture with superantigen cocktail-loaded Raji cells. The images in Fig. 6A show TCR (green) puncta spread around the cell as well as accumulated at the interface toward the Raji cell (cell demarcation shown in the DIC image). SNX17 (red) also showed puncta spread throughout the T cell and the Raji cell, with an accumulation of SNX17 puncta occurring in the T cell at the T-Raji interface. To further confirm SNX17 accumulation and localization with TCR at the synapse, we measured SNX17 and TCR fluorescence intensity across the T cell from the distal membrane, membrane located directly opposite of the synapse, to the T-Raji synapse using a line intensity profile (Fig. 6B, dotted line in Fig. 6A). Both TCR and SNX17 profiles show the highest overlapping spikes in fluorescence intensity occur at the synapse. We also measured the fluorescence intensity across the length the T cell surface at the immune synapse and found the highest spikes in SNX17 and TCR fluorescence intensity overlap, suggesting co-localization (Fig. 6B, yellow line in Fig. 6A). Next we measured if SNX17 and TCR are co-localized in our images at the immune synapse, by drawing a region of interest around the synapse for >20 T-Raji conjugates and measuring the co-localization coefficient. SNX17-TCR co-localization measured ~0.78 (Fig. 6C), which is similar to the co-localization coefficient seen in Fig. 1B and 1D. Interestingly, co-localization at the distal membrane showed little SNX17-TCR co-localization (Fig. 6C). The distal membranes lower SNX17-TCR co-localization could be attributed to lower SNX17 staining seen in all of our images at the distal membrane. In images taken of siSNX17 T cells placed in conjugate with Raji cells, very few conjugates were found to analyze for TCR localization at the synapse and the few conjugates we were able to find had SNX17 staining (data not shown). Overall, the accumulation of both TCR and SNX17 at the T-Raji synapse suggests that SNX17 plays a role in the transport and recycling of TCR at the synapse.

SNX17 FERM-domain is responsible in the surface expression of TCR and LFA-1

A few studies have found that the FERM-domain in SNX17 (Fig. 7A) is responsible for the transport and sorting of many receptors including the integrin β_1 (23, 24). The cytoplasmic region of CD3ε contains a highly conserved NPxY motif, while the β-chain of LFA-1 contains a highly conserved NPxF motif (Fig. 7B and C). To test SNX17 FERM-domain binding to the TCR and LFA-1, we used a previously described suppression/re-expression vector system (29) to deplete SNX17 in Jurkat T cells and simultaneously re-express either WT SNX17 or a FERM-domain mutant (L353W) that was previously shown to impair cargo binding (17). After transfecting Jurkat T cells with the indicated constructs, suppression and re-expression was confirmed by immunoblot (Supplemental Fig. S4A). The YFP$^+$

transfected cells were also analyzed by flow cytometry for cell surface expression of TCR and CD11a (Fig. 7D and 7E). Consistent with our prior results, depletion of SNX17 led to a loss of TCR and CD11a cell surface levels (Fig. 7D and 7E). Importantly, re-expression of wild type SNX17 restored TCR and CD11a cell surface levels back to those seen in shControl transfected Jurkat T cells. However, re-expression of the L353W FERM mutant did not restore TCR or CD11a cell surface levels, but in fact showed a similar MFI to cells depleted of SNX17 (Fig. 7D and 7E). Taken together, these data indicate that SNX17, through its FERM-domain, is critical to the trafficking of both the TCR and LFA-1 in T cells.

We next investigated whether SNX17 could interact with CD3ε. While GST-SNX17 was able to pull down CD3ε from unstimulated T cell lysates (Fig. 7F), the interaction between GST-SNX17 and CD3ε increased following stimulation with anti-CD3/CD28 (Fig. 7F), which is consistent with the co-localization data in Fig. 1B and D showing a significant increase in co-localization of SNX17 with TCR following T cell stimulation. Importantly, the L353W FERM-domain mutant did not interact with CD3ε, indicating that the FERM domain is required for their interaction (Fig. 7F). In addition, GST-SNX17 interacted with maltose-binding protein fusion proteins containing the cytoplasmic domain of either CD3ε or CD18 (Supplemental Figure S4B), suggesting that the interaction is direct. Taken together, these data indicate that SNX17 interacts with both CD3ε and CD18.

Discussion

The recycling and transport of receptors to the surface of T cells is crucial to formation of a functional immunological synapse and T cell activation (5, 7, 8). Multiple regulatory proteins, like Rab GTPases (5, 9–11); t-SNAREs: VAMP-3 (8), ti-VAMP (5) (12); IFT system protein IFT20 (7); and the ARP 2/3 activating WASH complex (13) have been discovered to play a key role in the trafficking of receptors, specifically the TCR, to the immune synapse during T cell activation. What remains unclear is how T cell activation and adhesion receptors are specifically sorted for trafficking to the immune synapse or cell surface. Herein we have determined that SNX17 participates in the trafficking of TCR and LFA-1 through the endosomal system and back to the plasma membrane. We found that the interaction of the SNX17 FERM-domain with TCR and LFA-1 leads to the specific sorting and trafficking of these receptors. In the absence of SNX17 as well as in mutation of the FERM-domain, we saw significant decreases in TCR and LFA-1 surface expression and T cell activation as a result of enhanced lysosomal degradation.

SNX17 is a member of a family of sorting nexins that contain a FERM domain, which includes SNX27 and SNX31. SNX17 has been implicated in integrin sorting in HeLa and embryonic stem cell lines (23, 24), but its role in immune cells, specifically $CD4^+$ T cells, is unknown. Our data show that GST-SNX17 could pull-down CD3ε and CD18 from T cell lysates and that this was dependent on the FERM domain, as mutation of the FERM domain (L353W) abrogated their interaction. Although CD18 does not contain an NPxY/NxxY motif, it does contain a highly conserved NPxF motif, with phenylalanine, an aromatic amino acid similar to the tyrosine residue, and integrin transport has been shown to continue when the tyrosine residue is mutated to phenylalanine in the NPxY motif of β_1-integrins

(30). Moreover, the FERM-domain of SNX17 has been shown to mediate binding and transport of the scavenger receptor FEEL-1/stabilin-1 by its NPxF motif (31) as well as binding to two of the NPxF motifs found in the adaptor protein Krev Interaction Trapped 1 (KRIT1) (32). We also find that there is a highly conserved NPxY motif in the CD3ε cytoplasmic tail, which is immediately distal to the Nck-SH3 binding site (RPPPVP) that was identified in CD3ε (33). Interestingly, the binding of the Nck-SH3 domain was dependent on the TCR being engaged by either MHC/peptide complexes or antibody crosslinking, suggesting that the CD3ε undergoes a conformational change to expose the Nck-SH3 binding site (33, 34). Significantly, we find that when compared to unstimulated cells, more CD3ε was co-precipitated with GST-SNX17 following TCR crosslinking, suggesting that the NPxY motif might also be more exposed when the TCR is engaged to allow SNX17 binding and thus recycling of the TCR. It should be mentioned that Mingueneau *et al*, showed that TCR surface expression and recycling remained unchanged when the proline-rich sequence of CD3ε was exchanged with a sequence from FcεR1γ that impacted the NPxY motif (35). It is unclear what the discrepancy is, but their recycling assays were performed in double positive thymocytes, which might use different mechanisms to recycle the TCR, or SNX17 is recognizing another protein associated with the TCR that is not CD3ε. While this remains a possibility, there are no NPxY motifs in either TCR α/β or the other CD3 complex components.

Our data also indicate that SNX17 localizes with the TCR and the α chain (CD11a) of integrin LFA-1. We consistently found that SNX17 co-localizes with TCR in both CD3/CD28 stimulated or unstimulated Jurkat T cells and primary human $CD4^+$ T cells. In contrast, only after CD3/CD28 stimulation of the T cell did SNX17 show increased co-localization with CD11a. The difference in localization of CD11a with SNX17 could be the result of differential compartmentalization or an overall change in LFA-1 surface expression during activation and migration. Naïve T cells have lower surface expression of LFA-1 than an activated or memory T cell (36). During activation, surface expression is increased and becomes dependent on recycling pathways. Activated T cells depend on LFA-1 recycling through the GTPases Rap1 (37, 38) and Rap2 (39) to assist in cell migration, as the leading edge of the T cell attaches, the rear detaches and the cell moves forward which requires dynamic turnover of LFA-1 (40). Additionally during T cell activation and immune synapse formation there is increased LFA-1 clustering at the peripheral SMAC (p-SMAC) due to specific signaling through the TCR (41) associated with actin polymerized endosomal trafficking (13, 42). It remains possible that after integrin activation, the LFA-1 heterodimer adopts an open conformation (43), which could possibly change the orientation of the β-chain's NPxF motif to allow for increased SNX17 interaction. The integrin conformational change could explain why we see less association of SNX17 with LFA-1 in naïve/unstimulated T cells. Further experiments are needed to address whether conformational changes during integrin activation provide an explanation for our results.

In stimulatory conditions, the role of SNX17 in receptor recycling and activation becomes more apparent. We show that in SNX17-deficient T cells there is decreased surface expression of TCR and LFA-1 and decreased activation and expression of TCR associated signaling molecules (pZAP-70) and markers of activation (CD69). These results are

consistent with our finding in the shSNX17 T cells, which form fewer conjugates. Lower surface expression of TCR and LFA-1 on the SNX17 depleted T cells interfere with successful engagement with APC receptors and result in poor immune synapse formation and abrogated receptor signaling and activation. In addition, T cells require continual turnover of receptors at the immune synapse to sustain signaling (3, 4, 7). In Fig. 5C and 5D we determined that without SNX17 the T cells lack the ability to recycle the TCR and CD11a back to the cell surface following receptor endocytosis. Our recycling data and our images showing SNX17 localized with the TCR at the immune synapse between a primary human $CD4^+$ T cell and SEE cocktail-loaded Raji cell suggest that SNX17 plays a significant role in the serial triggering and re-expression of endocytosed TCR at the immune synapse.

We have previously observed similar TCR localization with the lysosome in WASH depleted T cells (13), suggesting that WASH and SNX17 may work synergistically in the trafficking of the TCR. In addition, we as well as others have shown that integrins such as CD11a (13) and CD49e (44) are trafficked in a WASH-dependent fashion. It is of interest that SNX17 has been shown to be an important regulator of integrin trafficking in HeLa cells (18). Taken together, this might suggest a functional link between SNX17 and the WASH/retromer complexes in the recycling of integrin receptors. However, although a direct interaction between the WASH complex and SNX17 has not been reported, it is well appreciated that the SNX17 family member, SNX27, can directly interact with a component of the WASH complex and the retromer subunit VPS26 (23) thereby localizing cargo into this sorting domain. In fact, SNX27 also functions to regulate the trafficking of several integrins in HeLa cells (23), but whether SNX27 similarly participates in LFA-1 recycling in T cells remains to be established. Clearly, delineating a link between SNX17 and the WASH/retromer complexes, as well as examining the role of SNX27 in TCR and LFA-1 trafficking in T cells, will help shed light on how these different sorting nexin family members can promote integrin and or TCR recycling.

We also found that SNX17 prevented the localization of the TCR and CD11a with $LAMP1^+$ lysosomes. In fact, treating SNX17-depleted cells with cycloheximide, a protein translation inhibitor, resulted in a substantial loss of both receptors from the cell surface, suggesting that in the absence of new protein synthesis, these proteins are rapidly degraded. Consistent with this, in the absence of SNX17, TCR and CD11a co-localized with LAMP1 labeled lysosomes and degradation of both proteins was confirmed when we measured the amount of puncta present within the cell. Significantly, we could increase the intracellular levels of both TCR and CD11a by treating the cells with the lysosomal poison bafilomycin A1. Taken together, these data indicate that SNX17 is a key molecule required for the normal endosomal recycling of the TCR and LFA-1.

In conclusion, this work shows that SNX17 plays a significant role in the transport and recycling of human $CD4^+$ T cell receptors that are required for T cell activation. As SNX17 is a member of a family of FERM-domain containing proteins, the role of SNX27 in T cell biology, and specifically in the trafficking of CD3ε and CD18 remains to be determined. Moreover, further dissection of the functional interaction between this family of proteins and the WASH and retromer complexes in the trafficking of these receptors in T cells will

provide important insight into the mechanisms regulating T cell activation and immune synapse formation.

Supplementary Material

Refer to Web version on PubMed Central for supplementary material.

Acknowledgments

We specifically thank Dr. Christine Krawczak and other members of the Billadeau laboratory, past and present, for helpful discussions and advice.

This work was supported by the Mayo Foundation for Medical Research, NIH grant AI065474 to D.D.B., and NIH training grant 5T32AI007047-32 to D.G.O.

Abbreviations used in this article

SNX	sorting nexin
WASH	Wiskott Aldrich Syndrome protein and SCAR Homolog
LAMP1	lysosomal associated membrane protein 1
EEA	early endosomal antigen 1
TCR	T cell receptor
IS	immune synapse
FERM	4.1/ezrin/radixin/moesin
MFI	mean fluorescence intensity
GST	glutathione S-transferase
CHX	cyclheximide

References

1. Monks CR, Freiberg BA, Kupfer H, Sciaky N, Kupfer A. Three-dimensional segregation of supramolecular activation clusters in T cells. Nature. 1998; 395:82–86. [PubMed: 9738502]
2. Grakoui A, Bromley SK, Sumen C, Davis MM, Shaw AS, Allen PM, Dustin ML. The immunological synapse: a molecular machine controlling T cell activation. Science. 1999; 285:221–227. [PubMed: 10398592]
3. On the Dynamics of TCR:CD3 Complex Cell Surface Expression and Downmodulation. 2000. p. 1-11.
4. Lee K-H, Dinner AR, Tu C, Campi G, Raychaudhuri S, Varma R, Sims TN, Burack WR, Wu H, Wang J, Kanagawa O, Markiewicz M, Allen PM, Dustin ML, Chakraborty AK, Shaw AS. The immunological synapse balances T cell receptor signaling and degradation. Science. 2003; 302:1218–1222. [PubMed: 14512504]
5. Soares H, Henriques R, Sachse M, Ventimiglia L, Alonso MA, Zimmer C, Thoulouze M-I, Alcover A. Regulated vesicle fusion generates signaling nanoterritories that control T cell activation at the immunological synapse. J Exp Med. 2013; 210:2415–2433. [PubMed: 24101378]
6. Alcover A, Thoulouze M-I. Vesicle traffic to the immunological synapse: a multifunctional process targeted by lymphotropic viruses. Curr Top Microbiol Immunol. 2010; 340:191–207. [PubMed: 19960315]

7. Finetti F, Patrussi L, Masi G, Onnis A, Galgano D, Lucherini OM, Pazour GJ, Baldari CT. Specific recycling receptors are targeted to the immune synapse by the intraflagellar transport system. J Cell Sci. 2014; 127:1924–1937. [PubMed: 24554435]
8. Das V, Nal B, Dujeancourt A, Thoulouze M-I, Galli T, Roux P, Dautry-Varsat A, Alcover A. Activation-induced polarized recycling targets T cell antigen receptors to the immunological synapse; involvement of SNARE complexes. Immunity. 2004; 20:577–588. [PubMed: 15142526]
9. Echard A. Membrane traffic and polarization of lipid domains during cytokinesis. Biochem Soc Trans. 2008; 36:395–399. [PubMed: 18481967]
10. Patino-Lopez G, Dong X, Ben-Aissa K, Bernot KM, Itoh T, Fukuda M, Kruhlak MJ, Samelson LE, Shaw S. Rab35 and its GAP EPI64C in T cells regulate receptor recycling and immunological synapse formation. J Biol Chem. 2008; 283:18323–18330. [PubMed: 18450757]
11. Liu H, Rhodes M, Wiest DL, Vignali DA. On the dynamics of TCR:CD3 complex cell surface expression and downmodulation. Immunity. 2000; 13:665–675. [PubMed: 11114379]
12. Larghi P, Williamson DJ, Carpier J-M, Dogniaux S, Chemin K, Bohineust A, Danglot L, Gaus K, Galli T, Hivroz C. VAMP7 controls T cell activation by regulating the recruitment and phosphorylation of vesicular Lat at TCR-activation sites. Nat Immunol. 2013; 14:723–731. [PubMed: 23666293]
13. Piotrowski JT, Gomez TS, Schoon RA, Mangalam AK, Billadeau DD. WASH knockout T cells demonstrate defective receptor trafficking, proliferation, and effector function. Mol Cell Biol. 2013; 33:958–973. [PubMed: 23275443]
14. Worby CA, Dixon JE. Sorting out the cellular functions of sorting nexins. Nat Rev Mol Cell Biol. 2002; 3:919–931. [PubMed: 12461558]
15. Cullen PJ. Endosomal sorting and signalling: an emerging role for sorting nexins. Nat Rev Mol Cell Biol. 2008; 9:574–582. [PubMed: 18523436]
16. Carlton JG, Cullen PJ. Sorting nexins. Curr Biol. 2005; 15:R819–20. [PubMed: 16243015]
17. Ghai R, Bugarcic A, Liu H, Norwood SJ, Skeldal S, Coulson EJ, Li SS-C, Teasdale RD, Collins BM. Structural basis for endosomal trafficking of diverse transmembrane cargos by PX-FERM proteins. Proc Natl Acad Sci USA. 2013; 110:E643–52. [PubMed: 23382219]
18. Steinberg F, Heesom KJ, Bass MD, Cullen PJ. SNX17 protects integrins from degradation by sorting between lysosomal and recycling pathways. J Cell Biol. 2012; 197:219–230. [PubMed: 22492727]
19. van Kerkhof P, Lee J, McCormick L, Tetrault E, Lu W, Schoenfish M, Oorschot V, Strous GJ, Klumperman J, Bu G. Sorting nexin 17 facilitates LRP recycling in the early endosome. EMBO J. 2005; 24:2851–2861. [PubMed: 16052210]
20. Stockinger W, Sailler B, Strasser V, Recheis B, Fasching D, Kahr L, Schneider WJ, Nimpf J. The PX-domain protein SNX17 interacts with members of the LDL receptor family and modulates endocytosis of the LDL receptor. EMBO J. 2002; 21:4259–4267. [PubMed: 12169628]
21. Burden JJ, Sun X-M, García ABG, Soutar AK. Sorting motifs in the intracellular domain of the low density lipoprotein receptor interact with a novel domain of sorting nexin-17. J Biol Chem. 2004; 279:16237–16245. [PubMed: 14739284]
22. Tseng H-Y, Thorausch N, Ziegler T, Meves A, Fässler R, Böttcher RT. Sorting nexin 31 binds multiple β integrin cytoplasmic domains and regulates β1 integrin surface levels and stability. J Mol Biol. 2014
23. Steinberg F, Gallon M, Winfield M, Thomas EC, Bell AJ, Heesom KJ, Tavaré JM, Cullen PJ. A global analysis of SNX27-retromer assembly and cargo specificity reveals a function in glucose and metal ion transport. Nat Cell Biol. 2013; 15:461–471. [PubMed: 23563491]
24. Böttcher RT, Stremmel C, Meves A, Meyer H, Widmaier M, Tseng H-Y, Fässler R. Sorting nexin 17 prevents lysosomal degradation of β1 integrins by binding to the β1-integrin tail. Nat Cell Biol. 2012; 14:584–592. [PubMed: 22561348]
25. Knauth P, Schlüter T, Czubayko M, Kirsch C, Florian V, Schreckenberger S, Hahn H, Bohnensack R. Functions of sorting nexin 17 domains and recognition motif for P-selectin trafficking. J Mol Biol. 2005; 347:813–825. [PubMed: 15769472]

26. Rincón E, Sáez de Guinoa J, Gharbi SI, Sorzano COS, Carrasco YR, Mérida I. Translocation dynamics of sorting nexin 27 in activated T cells. J Cell Sci. 2011; 124:776–788. [PubMed: 21303929]
27. Sullivan BM, Coscoy L. Downregulation of the T-cell receptor complex and impairment of T-cell activation by human herpesvirus 6 u24 protein. J Virol. 2008; 82:602–608. [PubMed: 17977973]
28. Ham H, Guerrier S, Kim J, Schoon RA, Anderson EL, Hamann MJ, Lou Z, Billadeau DD. Dedicator of cytokinesis 8 interacts with talin and Wiskott-Aldrich syndrome protein to regulate NK cell cytotoxicity. J Immunol. 2013; 190:3661–3669. [PubMed: 23455509]
29. Gomez TS, Billadeau DD. A FAM21-containing WASH complex regulates retromer-dependent sorting. Dev Cell. 2009; 17:699–711. [PubMed: 19922874]
30. Maginnis MS, Mainou BA, Derdowski A, Johnson EM, Zent R, Dermody TS. NPXY motifs in the beta1 integrin cytoplasmic tail are required for functional reovirus entry. J Virol. 2008; 82:3181–3191. [PubMed: 18216114]
31. Adachi H, Tsujimoto M. Adaptor protein sorting nexin 17 interacts with the scavenger receptor FEEL-1/stabilin-1 and modulates its expression on the cell surface. Biochim Biophys Acta. 2010; 1803:553–563. [PubMed: 20226821]
32. Stiegler AL, Zhang R, Liu W, Boggon TJ. Structural determinants for binding of Sorting Nexin 17 (SNX17) to the cytoplasmic adaptor protein Krev Interaction Trapped 1 (KRIT1)*. J Biol Chem. 2014 jbc.M114.584011.
33. Gil D, Schamel WWA, Montoya M, Sanchez-Madrid F, Alarcón B. Recruitment of Nck by CD3 epsilon reveals a ligand-induced conformational change essential for T cell receptor signaling and synapse formation. Cell. 2002; 109:901–912. [PubMed: 12110186]
34. Szymczak AL, Workman CJ, Gil D, Dilioglou S, Vignali KM, Palmer E, Vignali DAA. The CD3epsilon proline-rich sequence, and its interaction with Nck, is not required for T cell development and function. J Immunol. 2005; 175:270–275. [PubMed: 15972658]
35. Mingueneau M, Sansoni A, Grégoire C, Roncagalli R, Aguado E, Weiss A, Malissen M, Malissen B. The proline-rich sequence of CD3epsilon controls T cell antigen receptor expression on and signaling potency in preselection CD4+CD8+ thymocytes. Nat Immunol. 2008; 9:522–532. [PubMed: 18408722]
36. Hviid L, Odum N, Theander TG. The relation between T-cell expression of LFA-1 and immunological memory. Immunology. 1993; 78:237–243. [PubMed: 8097182]
37. Dustin ML, Bivona TG, Philips MR. Membranes as messengers in T cell adhesion signaling. Nat Immunol. 2004; 5:363–372. [PubMed: 15052266]
38. Kinashi T, Katagiri K. Regulation of immune cell adhesion and migration by regulator of adhesion and cell polarization enriched in lymphoid tissues. Immunology. 2005; 116:164–171. [PubMed: 16162265]
39. Stanley P, Tooze S, Hogg N. A role for Rap2 in recycling the extended conformation of LFA-1 during T cell migration. Biol Open. 2012; 1:1161–1168. [PubMed: 23213397]
40. Vicente-Manzanares M, Choi CK, Horwitz AR. Integrins in cell migration--the actin connection. J Cell Sci. 2009; 122:199–206. [PubMed: 19118212]
41. Cairo CW, Mirchev R, Golan DE. Cytoskeletal regulation couples LFA-1 conformational changes to receptor lateral mobility and clustering. Immunity. 2006; 25:297–308. [PubMed: 16901728]
42. Nolz JC, Medeiros RB, Mitchell JS, Zhu P, Freedman BD, Shimizu Y, Billadeau DD. WAVE2 regulates high-affinity integrin binding by recruiting vinculin and talin to the immunological synapse. Mol Cell Biol. 2007; 27:5986–6000. [PubMed: 17591693]
43. Smith A, Stanley P, Jones K, Svensson L, McDowall A, Hogg N. The role of the integrin LFA-1 in T-lymphocyte migration. Immunol Rev. 2007; 218:135–146. [PubMed: 17624950]
44. Zech T, Calaminus SDJ, Caswell P, Spence HJ, Carnell M, Insall RH, Norman J, Machesky LM. The Arp2/3 activator WASH regulates α5β1-integrin-mediated invasive migration. J Cell Sci. 2011; 124:3753–3759. [PubMed: 22114305]

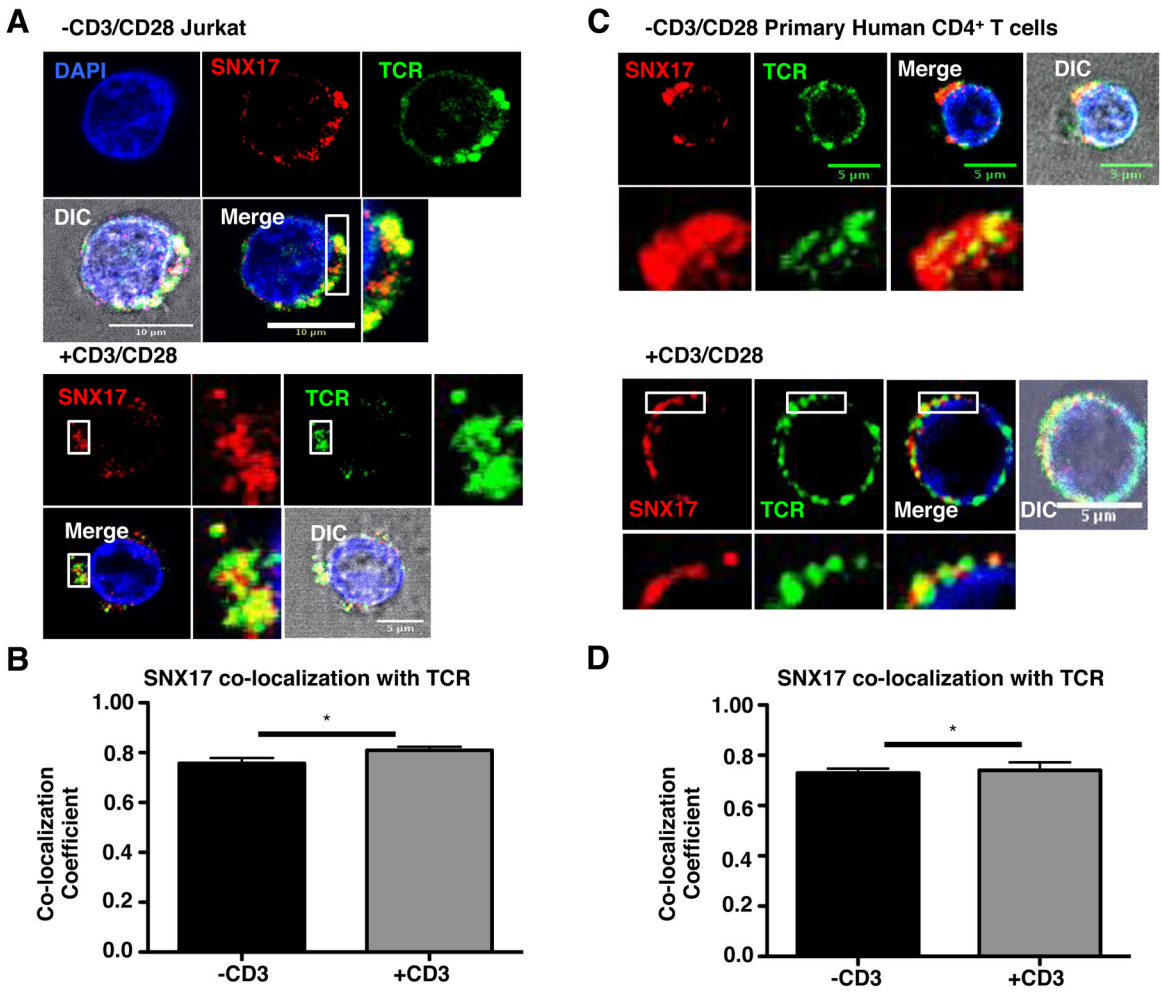

Figure 1. SNX17 co-localizes with TCR in activated CD4$^+$ T cells

(A) Unstimulated or anti-CD3/CD28 stimulated Jurkat T cells, following the T cell stimulation protocol in the Materials and Methods, were labeled with antibodies against TCR using the endocytosis assay, fixed, and then labeled with antibodies against SNX17 and nuclear stained with Hoechst for immunofluorescence (IF). (B) Pearson's coefficient was measured from images in A using ZEN (Carl Zeiss). (C) Unstimulated or anti-CD3/CD28 stimulated primary human CD4$^+$ T cells labeled with antibodies against TCR using the endocytosis assay, fixed, and then antibody labeled against SNX17 for IF. (D) Pearson's coefficient was measured from images in C using ZEN. Zoom images are demarcated by the white box in adjacent image. Differential interference contrast (DIC) image used to demarcate the outline of the cell. For each condition, >20 individual cells were imaged from each of 3 separate imaging experiments. Images were collected with 100x oil objective. Scale bars, 5 and 10 μm. Bars represent mean ± SEM. Horizontal lines indicate statistical comparison between groups, *p≤0.05.

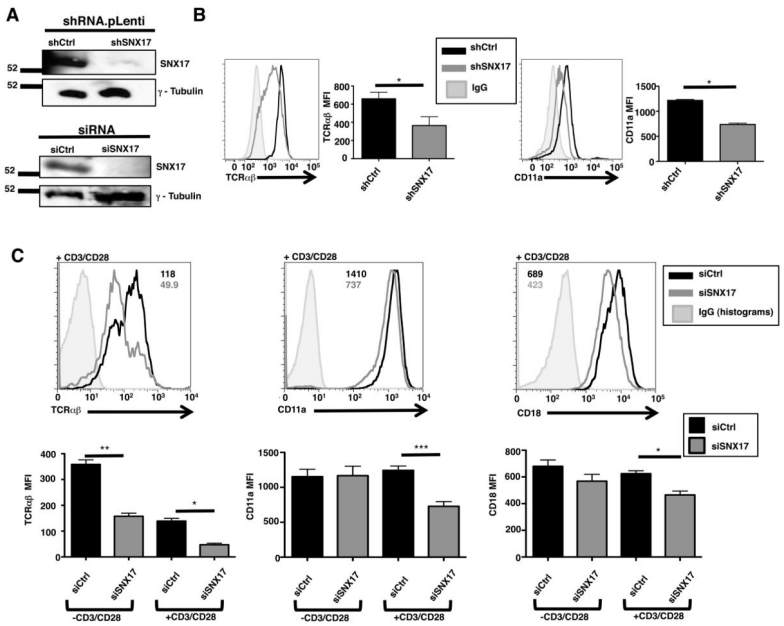

Figure 2. SNX17 knockdown in CD4$^+$ T cells leads to decreased TCR and LFA-1 surface expression

(A) Top, protein lysates prepared from lentiviral vector shControl and shSNX17 Jurkat T cells were immunoblotted for SNX17 and γ-Tubulin (as a loading control). Bottom, protein lysates prepared from siRNA Control and siSNX17 primary human CD4$^+$ T cells were immunoblotted for SNX17 and γ-Tubulin (as a loading control). (B) shControl (black line) and shSNX17 (gray line) Jurkat T cells were antibody stained for surface TCRαβ and CD11a and analyzed using flow cytometry. Histogram and bar graphs are representative of eight separate experiments. (C) Unstimulated and anti-CD3/CD28 stimulated siControl (black) and siSNX17 (gray) primary human CD4$^+$ T cells were surfaced labeled for TCRαβ (left), CD11a (center), and CD18 (right) were analyzed using flow cytometry. Histograms and graphs are representative of four separate experiments. Bars represent mean ± SEM. Horizontal lines indicate statistical comparison between groups, *p≤0.05, **p≤0.01 and ***p≤0.0005.

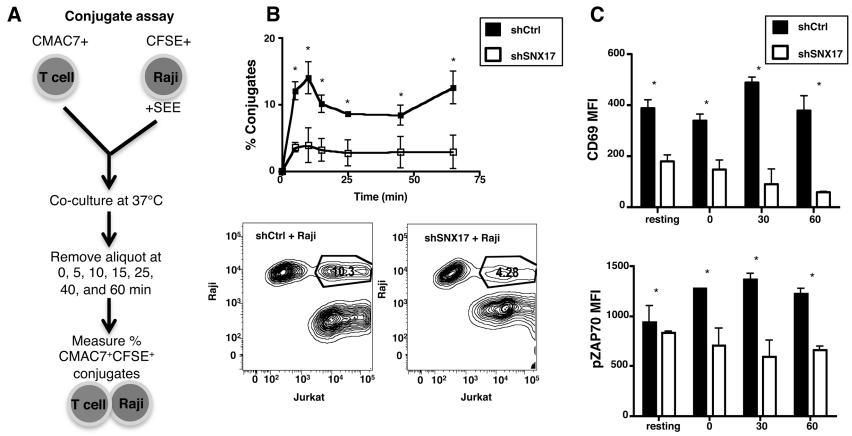

Figure 3. SNX17 knockdown leads to decreased conjugate formation and activation

(A) Diagram of the Conjugate assay protocol. (B) Percent conjugates were measured and contour plots made for shControl (black box) and shSNX17 (white box) Jurkat T cells in culture with +SEE loaded Raji cells as shown in A. (C) ShControl (black) and shSNX17 (white) Jurkat T cells in the conjugate assay were antibody labeled for CD69 and permeabilized and phospho-labeled for pZAP-70 and analyzed using flow cytometry. B and C are representative of four separate experiments. Bars represent mean ± SEM. *p≤0.0005.

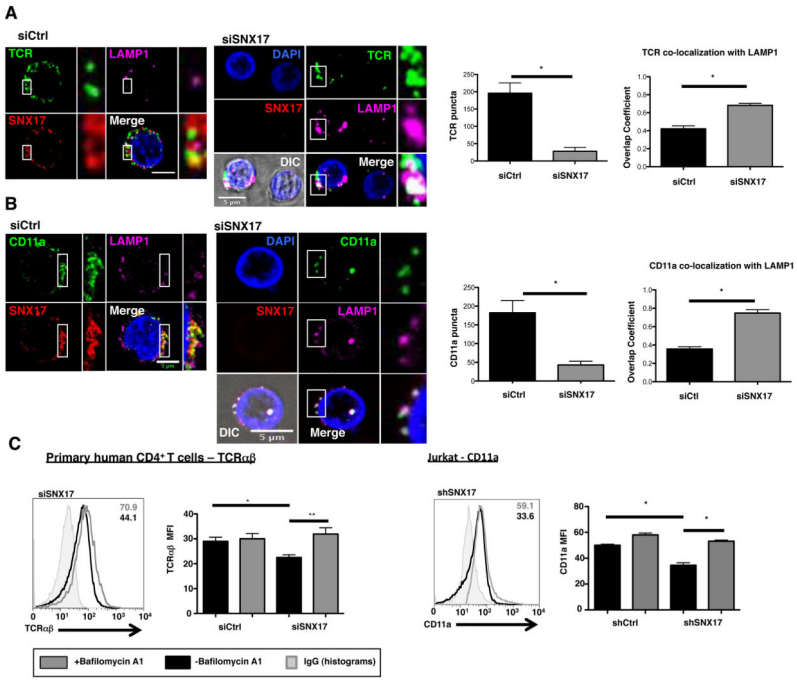

Figure 4. SNX17 prevents the localization of TCR and CD11a into lysosomes following endocytosis

(A) Antibody-stimulated siControl and siSNX17 primary human $CD4^+$ T cells were cultured with primary antibody against TCR following the endocytosis assay, fixed, and labeled with antibodies against SNX17, LAMP1, and nuclear stained with Hoechst for IF. (B) Antibody-stimulated siControl and siSNX17 primary human $CD4^+$ T cells were cultured with primary antibody against CD11a following the endocytosis assay, fixed, and labeled with antibodies against SNX17, LAMP1, and nuclear stained with Hoechst for IF. Images from A and B were analyzed for TCR and CD11a puncta number and co-localization with LAMP1 using overlap coefficient in ZEN (Carl Zeiss). (C) siControl and siSNX17 primary human $CD4^+$ T cells and Jurkat T cells +/− 100 nM Bafilomycin A1 were cultured for 18 hrs and analyzed for TCR and CD11a MFI using flow cytometry. Bar graphs in C based on 3 separate experiments. Zoomed images are demarcated by the white box and dashed lines toward the adjacent image. Differential interference contrast (DIC) image used to demarcate the outline of the cell. For each condition, >20 individual cells were imaged from each of 2 separate imaging experiments. Images were collected with 100x oil objective. Scale bars, 5 μm. Bars represent mean ± SEM. Horizontal lines indicate statistical comparison between groups, *p≤0.05, ***p*≤0.01.

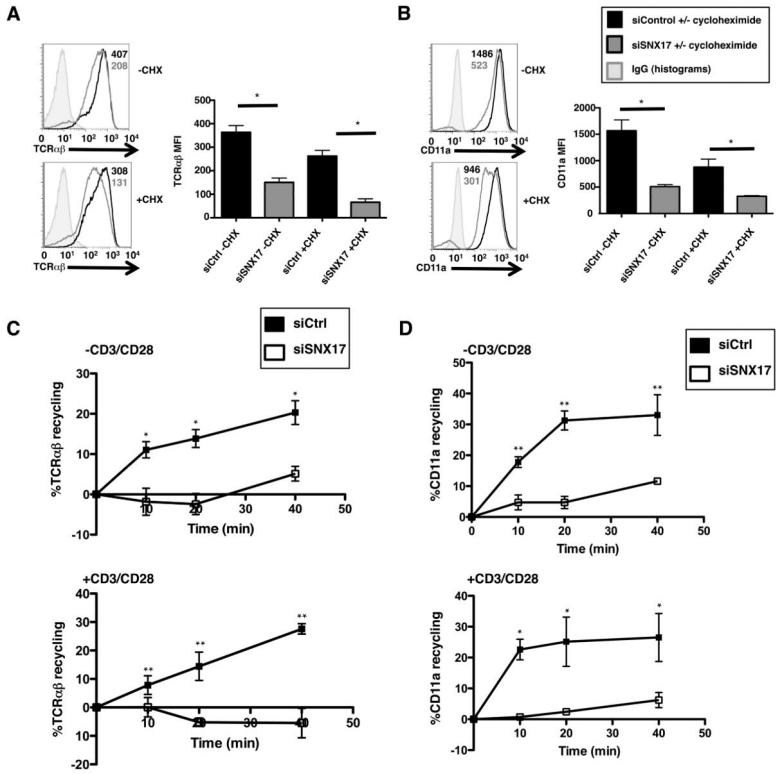

Figure 5. SNX17 is involved in TCR and LFA-1 receptor recycling in T cells

(A, B) Flow cytometric analysis of CD3/CD28 antibody stimulated siControl (black) and siSNX17 (gray) primary human $CD4^+$ T cells treated with 20 μg/ml cycloheximide for 24 hrs and then surfaced labeled for TCRαβ and CD11a. (C) TCRαβ and (D) CD11a recycling was measured in siControl and siSNX17 primary human $CD4^+$ T cells using acid stripping as described in the Materials and Methods. A–D are representative examples of 3 separate experiments. Bars represent mean ± SEM. Horizontal lines indicate statistical comparison between groups, *$p \leq 0.05$, **$p \leq 0.0005$.

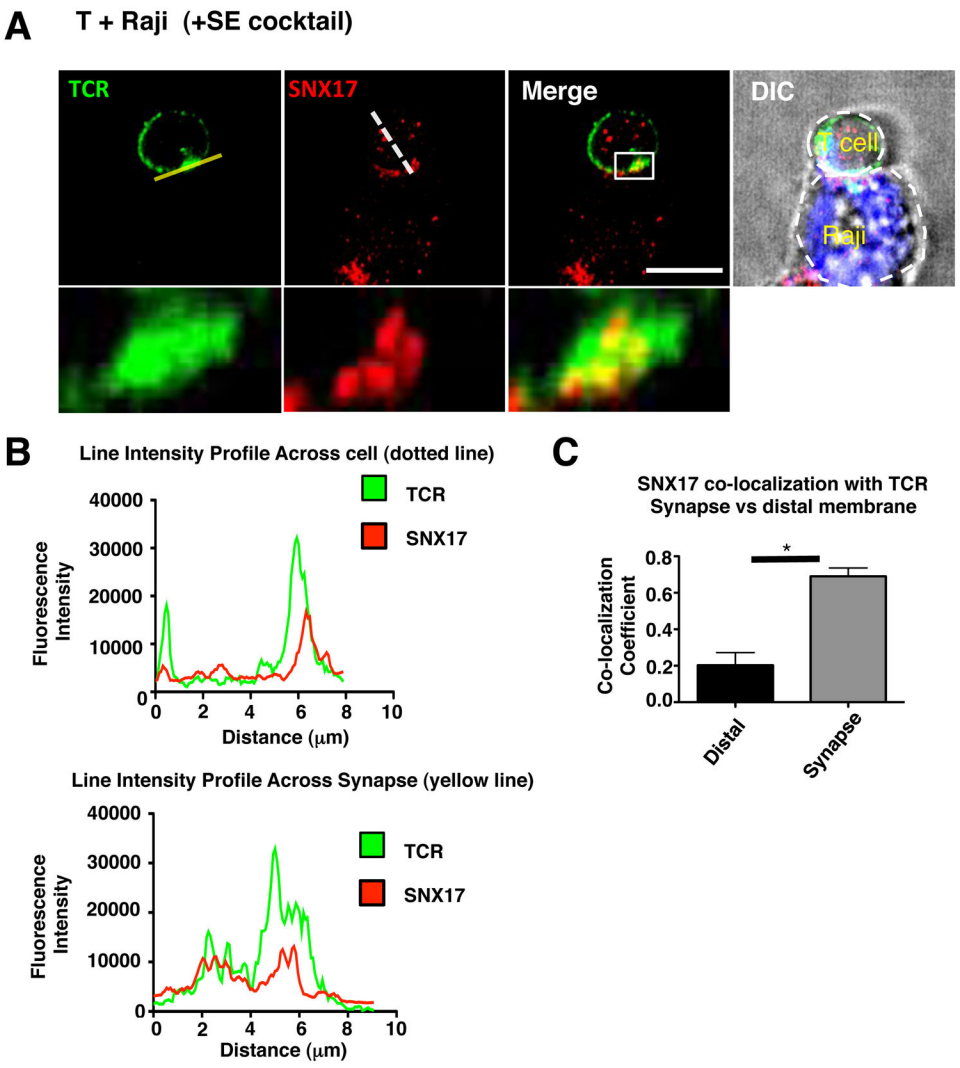

Figure 6. SNX17 localizes with the TCR at the immune synapse

(A) Primary human $CD4^+$ T cells were placed in co-culture with CMAC7 stained SE cocktail loaded Raji cells then fixed and labeled with antibodies against TCR and SNX17 for IF. (B) Line intensities profiles were created from the yellow line (bottom graph) and the dotted line (top graph) in images from A using FIJI. (C) Images from A were analyzed for the co-localization of SNX17 with the TCR at the T cell-Raji interface and at the T cell distal membrane using Pearson's co-localization coefficient in ZEN. Zoomed images are demarcated by the white box in the adjacent image. Differential interference contrast (DIC) image used to demarcate the outline of the cell. For A and C, >20 T cell-Raji conjugates were imaged and analyzed from each of 3 separate imaging experiments. Images were collected with 100x oil objective. Scale bars, 10 μm. Bars represent mean ± SEM. Horizontal lines indicate statistical comparison between groups, *p≤0.05.

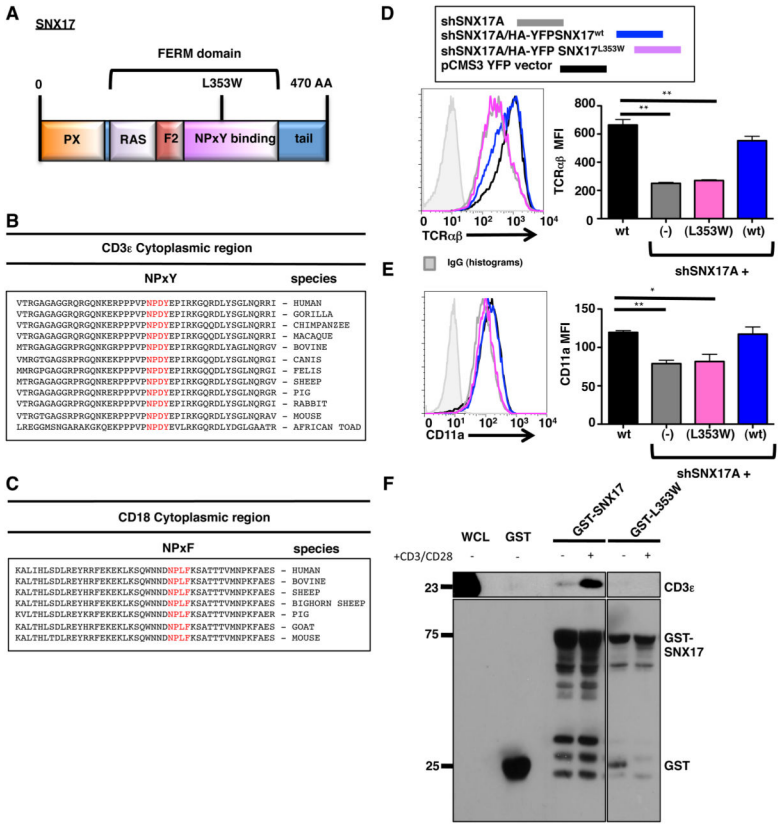

Figure 7. The SNX17 FERM-domain binds and traffics TCR and LFA-1

(A) Diagram of SNX17. (B) Peptide alignment of the cytoplasmic region of CD3ε. (C) Peptide alignment of the cytoplasmic region of CD18. (D) Transfected pCMS3. YFP vector control (black), shSNX17A (gray), shSNX17A/HA-YFP SNX17^{WT} (blue), and shSNX17A/HA-YFP SNX17^{L353W} (magenta) Jurkat T cells were surfaced labeled for TCRαβ and YFP^{+} cells were analyzed using flow cytometry. (E) Transfected pCMS3 YFP vector control (black), shSNX17A (gray), shSNX17A/HA-YFP SNX17^{wt} (blue), and shSNX17A/HA-YFP SNX17^{L353W} (magenta) Jurkat T cells were surfaced labeled for CD11a and YFP^{+} cells were analyzed using flow cytometry. (F) GST-pull down assay using whole cell lysates from unstimulated or anti-CD3/CD28 treated primary human CD4^{+} T cells. The pull-down was performed with GST only control, GST-SNX17, or GST-SNX17 (L353W) mutant and immunoblotted for CD3ε and GST. The results in D and E are representative of four separate experiments, while F is representative of 3 separate immunoblot experiments. Bars represent mean ± SEM. Horizontal lines indicate statistical comparison between groups, *p≤0.05, **p≤0.005.